



ELSEVIER

Available online at [www.sciencedirect.com](http://www.sciencedirect.com)

ScienceDirect

Procedia Engineering 2 (2010) 1253–1262

---

---

**Procedia  
Engineering**

---

---

[www.elsevier.com/locate/procedia](http://www.elsevier.com/locate/procedia)

Fatigue 2010

# On the distributions of fatigue lives and defect-sizes in the die-cast magnesium alloy AZ91

S. Ishihara<sup>\*</sup>, S. Yoshifuji, T. Namito and T. Goshima*Department of Mechanical Engineering, University of Toyama, Japan*

Received 27 February 2010; revised 10 March 2010; accepted 15 March 2010

---

## Abstract

In this study, fatigue tests were carried out using a diecast Mg alloy AZ91 to study the distribution of fatigue lives under constant stress amplitudes. During the fatigue process of the diecast Mg alloy, cracks initiated from the casting defect existing inside of the specimen, and then propagated prior to final failure of the specimen. The probabilistic distributions of the defects densities, of the defect sizes, and of the spatial positions of the defects were investigated experimentally in detail. The distributions of the fatigue lives of the diecast Mg alloys under the constant stress amplitudes were evaluated using the Monte-Carlo simulation, in which the random numbers corresponding to the above probabilistic distributions for the casting defects are used. There was a good fit between the evaluated distribution of the fatigue lives by the computer simulation and the experimental one. An increase of scatter in the distribution of the fatigue life with lowering of the stress amplitude could also be predicted using the simulation.

© 2010 Published by Elsevier Ltd. Open access under [CC BY-NC-ND license](http://creativecommons.org/licenses/by-nc-nd/3.0/).*Keywords:* Diecast, magnesium alloy, Distribution of fatigue lives, Casting defect, Weibull distribution

---

## 1. Introduction

The diecast magnesium alloys are now used in various industrial products, such as car components and structural materials and so on, since they have a good productivity, a superior specific strength, and high dimensional accuracy [1]. Further the production cost of the diecast alloy is comparatively low. In the diecast process, casting defects yield in great numbers, since molten metal is ejected into the die inside at high speed and at high pressure. Reliability for the fatigue strength of the diecast material is doubtful, because they are influenced by existences of the casting defects. Horstemeyer et al. [2] conducted high cycle fatigue tests on the diecast AZ91 Mg alloy, and reported that casting defects and microstructures cause the strong effect on the distribution of the fatigue lives and crack propagation behavior. Avalle et al. [3] investigated the effect of the casting defect on the fatigue strength for the diecast aluminum alloy. They reported that cracks were initiated early from the gas cavities during the fatigue process, and reduced the fatigue lives of the material. Both the size and the generation place of the casting defect are responsible for the fatigue strength. Murugan et al. [4] reported that the casting defect strongly influences the distribution of the fatigue lives of the casting AZ91 magnesium alloy. Fatigue cracks were clarified to be initiated from the casting defects.

---

<sup>\*</sup> Corresponding author. Tel.: +81-76-445-6771; fax: +81-76-445-6771.

E-mail address: [ishi@eng.u-toyama.ac.jp](mailto:ishi@eng.u-toyama.ac.jp).

As reviewed above, it was clarified that the die casting defects strongly influence the fatigue lives of the cast or the diecast magnesium alloy. However, there are still many unknowns on the distribution of the fatigue lives for the diecast magnesium alloys. Further the method that can quantitatively evaluate the fatigue lives of the diecast magnesium alloy has not been provided, and is now strongly required. This situation constitutes a limiting factor for the application of the diecast magnesium alloy to the structural members.

In the present study, fatigue tests were performed on the diecast magnesium alloy AZ91 to study its S-N curve as well as distribution of the fatigue lives. During the fatigue process of the material, it was observed that final failure of the specimen was caused by the crack initiation from the casting defects that are located at 50-300  $\mu\text{m}$  in depth from the specimen surface. So, the probabilistic distributions of the density, size, and position of the casting defects within the specimens were investigated in detail. Distribution of the fatigue lives was evaluated considering the Probabilistic distribution of the casting defects. The estimated distributions corresponded well with the experimental one.

## 2. Materials, specimen and experimental procedures

### 2.1. Materials and specimen

The material used was a diecast magnesium alloy AZ91. Its chemical compositions are listed in Table 2. The mechanical properties of the material are follows: Tensile strength =211.7 MPa, Yield strength = 183 MPa (0.2 % proof stress), Elongation = 1.34 %, Hardness = HV92. The sandglass-type round-bar specimen was used in the present study. The shape and dimensions of the specimen are shown in Fig. 1, with a gauge diameter 6.0 mm, and a gripping diameter 10mm.

Table 1 Chemical compositions of the material used [mass %]

Al	Zn	Mn	Fe	Si	Cu	Ni	Mg
8.9	0.69	0.18	0.0022	0.03	0.001	0.0005	Bal.

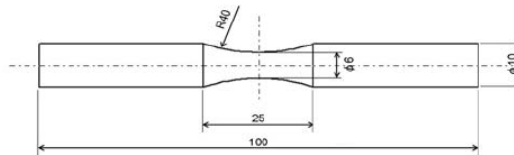


Fig.1 Specimen shapes and dimensions used in the test [mm]

### 2.2 Experimental procedures

#### (a) Fatigue test

Fatigue tests and crack propagation experiments on the diecast magnesium alloy AZ91 were conducted using a cantilever type rotating bending fatigue machine (four-run type). The tests were conducted at stress frequency  $f = 30$  Hz in laboratory air at a room temperature 15-28 degree C and relative humidity of 30-60%. The distributions of the fatigue lives were investigated using 20 specimens at constant stress amplitudes, 80, 100 and 120 MPa. The replication technique was employed to study the short fatigue crack propagation behavior. The fatigue tests were interrupted at the constant intervals to collect the replicas of the specimen surface during the fatigue process. Then the replicas were examined to measure the crack lengths using an optical microscope with a magnification of 200. The maximum stress intensity factor  $K_{\max}$  was evaluated using the following expression (1) with an assumption that the crack shape is semicircular, where  $Y$  is a correction factor with a value 0.73 for the semicircular shaped surface crack,  $a$  is a half crack length, and  $\sigma_a$  is a stress amplitude.

$$K_{\max} = Y\sigma_a\sqrt{\pi a} \quad (1)$$

(b) Fractography

The fracture surfaces for the 60 specimens tested (three stress amplitudes, and 20 specimens for a constant stress amplitude) were observed using a scanning electron microscope (SEM, Hitachi Co Ltd., TM-1000) to examine positions and sizes of the casting defects that led to final failure of the specimens.

(c) Probabilistic distribution of the casting defects

After polishing the specimen's cross sections into mirror like finish, ten visual fields with an area of 1.5 mm<sup>2</sup> for each specimen were examined using an optical microscope (Olympus Co. Ltd., BX51M) to investigate the densities and sizes of the casting defects. The image data processing software system (Mitani Co. LTD, Win ROOF) was used to analyze the above casting defects. Number of the data analyzed is above 100,000. The cross sections of the 60 fractured specimens were examined using the above method. Figure 2 shows an example of the appearance of the cross section of the specimen. A many distributed casting defects can be found in the cross section.

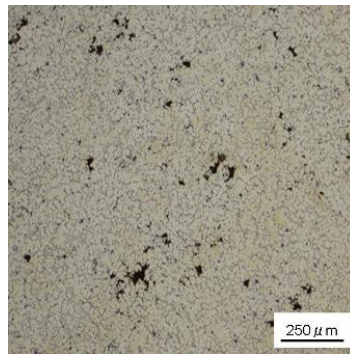
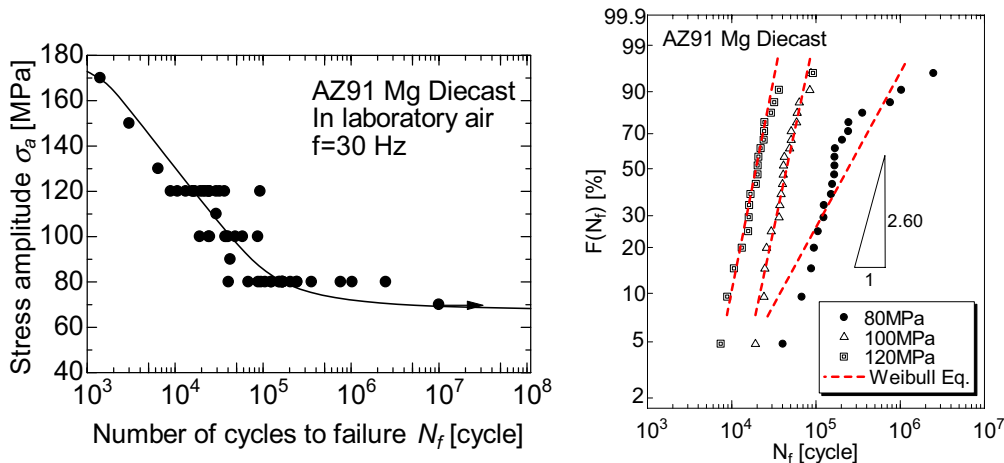


Fig. 2 An example of the cross section of the specimen showing existences of the many casting defects.

3. Experimental results

3.1 Distribution of fatigue lives

Figure 3(a) shows the relation between stress amplitude  $\sigma_a$  and number of cycles to failure  $N_f$  for the diecast magnesium alloy. This relation was obtained by the rotating bending fatigue tests. The data with arrow in this figure indicates that the specimen was not broken until the cycles. The distributions of fatigue lives at the constant stress



(a) S-N curve of AZ91 die-cast

(b) Distribution of fatigue lives plotted on the Weibull.

Fig. 3 Distribution of fatigue lives of AZ91 diecast.

amplitudes were studied using 20 specimens at the constant stress amplitudes. Figure 3(b) shows the Weibull distributions of fatigue lives at the constant stress amplitudes.

$$F(N_f) = 1 - \exp\left\{-\left(\frac{N_f}{\alpha}\right)^m\right\} \quad (2)$$

The figure shows that extents in the distributions for the higher stress amplitudes 100 and 120 MPa are almost identical to each other. However the scatter in the distribution of fatigue lives becomes larger at the lower stress amplitude of 80 MPa as compared with those at the higher stress amplitudes. The fatigue life distribution at 80 MPa is seen to be composed of the two different distributions. The boundary between them is about 70% of the cumulative probability.

The broken lines in Fig. 2(b) are the approximate ones for the distribution of fatigue lives by the two parameter Weibull distribution Eq. (2). The parameters  $\alpha$  and  $m$  were determined to meet the maximum correlation coefficient. These values for each of stress amplitude are listed in Table 2.

Table 2 Values of two parameters,  $\alpha$ ,  $m$

$\sigma_a$	$\alpha$	$m$
80 MPa	322642	0.91
100 MPa	51030	2.60
120 MPa	23515	2.43

### 3.2 Crack propagation behavior

Figure 4 shows the relation between the rate of fatigue crack propagation on the specimen surface  $da/dN$  and maximum stress intensity factor  $K_{max}$ . The solid line in the figure is an approximate curve to the experimental data, and is expressed by the next expression Eq. (3), where the value of  $0.52 \text{ MPa}\sqrt{\text{m}}$  indicates the threshold for the crack propagation.

$$\frac{da}{dN} = 6.0 \times 10^{-9} (K_{max} - 0.52)^2 \quad (3)$$

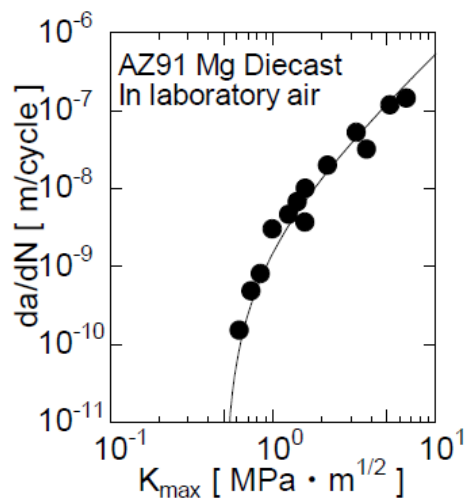


Fig. 4 Relationship between  $da/dN$  and  $K_{max}$  for surface crack.

### 3.3 Cracks initiation behavior during the fatigue process

Figure 5(a) and 5(b) show the fracture surfaces for the specimens with the shortest and longest fatigue lives among the twenty fatigue failed specimens at the constant stress amplitude of 80 MPa, respectively. The white dotted curves in these figures show the casting defects from which the fatigue cracks initiated during the fatigue process. In the specimen showing the shortest fatigue life (Fig. 5(a)), the casting defect is clearly larger as compared with that in the specimen with the longest fatigue life (Fig. 5(b)). The depths were determined from the fracture surfaces of the 60 specimens using the scanning electron microscope (SEM). The sources of the fatigue cracks were clarified as the casting defects inside of the specimens regardless of the stress amplitudes. Their depths range from 50  $\mu\text{m}$  to 300  $\mu\text{m}$  from the specimen surfaces. The depth of the casting defects decreased with a decrease in the stress amplitude. In the next section, the probabilistic distribution of these casting defects will be described in detail.

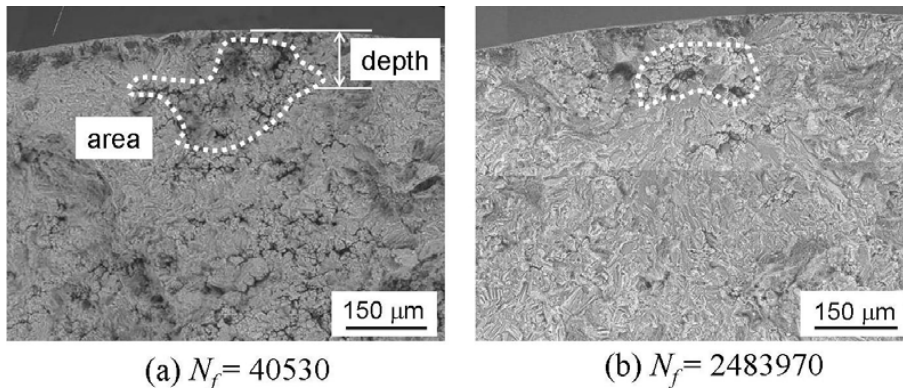


Fig. 5 SEM micrographs of crack initiation on the fracture surface

### 3.4 Spatial distribution of the casting defects

The probabilistic distribution for the casting defects was investigated. The sixty fatigue-failed specimens were used for this purpose. Figure 6 shows the distributions of sizes (area) of the casting defects in the cross section of the specimen. The data determined in the ringed regions with a different radius from the center of the specimen are plotted in the figure. As can be seen from the figure, there are no effects of the radius from the center of the specimen on these size distributions. In other words, the casting defects distribute spatially in a random manner. So the probabilistic distributions of the casting defects were determined in the whole cross section of the specimen.

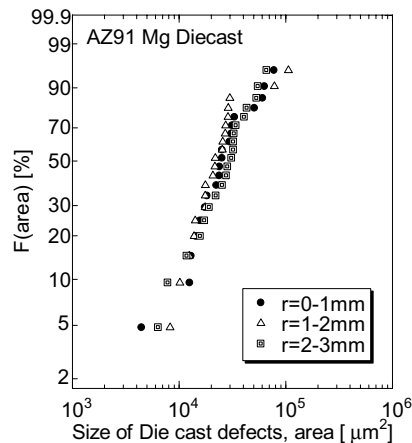


Fig. 6 Size (area) distribution of the casting defects in the ringed regions with a different radius from the center of the specimen

Weibull distributions of the sizes and densities for the die-casting defects in the entire cross section of the specimen are shown in Figs. 7(a) and 7(b), respectively. Defects with areas larger than  $50 \mu\text{m}^2$  were only measured, and plotted in these figures. The dotted curves in these figures show the fitted curves to the experimental data that are represented by the three-parameters (Eq. (4)) and two-parameters (Eq. (5)) Weibull distributions. The values of parameters used are listed in Table 3.

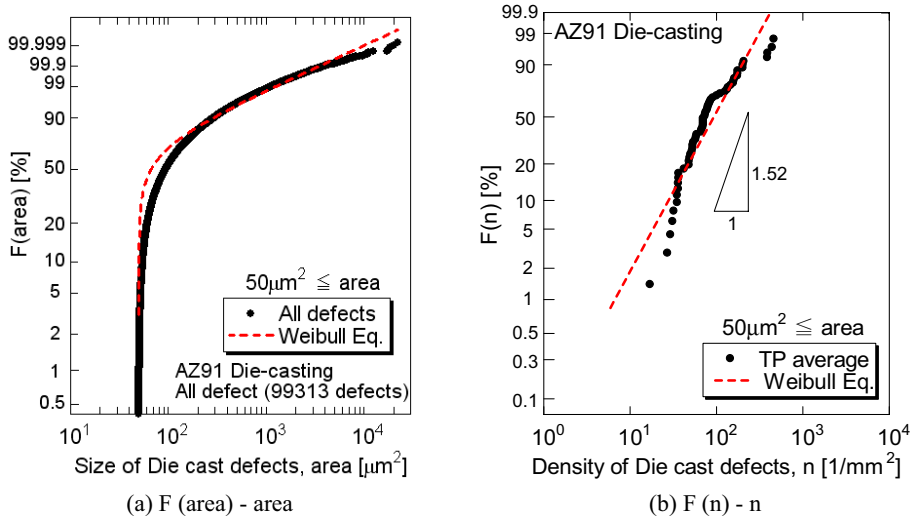


Fig. 7 Weibull distribution of casting defects

$$F(\text{area}) = 1 - \exp\left\{-\left(\frac{\text{area} - \gamma}{\alpha}\right)^m\right\} \tag{4}$$

$$F(n) = 1 - \exp\left\{-\left(\frac{n}{\alpha}\right)^m\right\} \tag{5}$$

Table 3 Weibull parameter

	$\alpha$	$\gamma$	m
F(area)	31.08	50	0.41
F(n)	114.73	-	1.52

### 3.5 Deterministic evaluation of fatigue lives

The areas of the casting defects (*area*) from which fatigue cracks initiated were determined using scanning electron microscope (SEM) by observing the fracture surfaces for the sixty specimens tested. Substituting these *areas* into the next equation (6) [5], the initial maximum stress intensity factors  $K_{i\text{max}}$  were evaluated with assumption that these casting defects are initial cracks.  $\sigma_{al}$  is a local stress at the center of the die-casting defect, and

can be evaluated using equation (7), where  $d_0$  is a specimen diameter and  $depth$  is a distance which is defined as in Fig. 4.

$$K_{i_{max}} = 0.5\sigma_{al}\sqrt{\pi\sqrt{area}} \tag{6}$$

$$\sigma_{al} = \sigma_a \left(1 - \frac{2depth}{d_0}\right) \tag{7}$$

Figure 8 shows the log-log plot between the initial maximum stress intensity factors  $K_{i_{max}}$  and fatigue lives  $N_f$  for three stress amplitudes, 80, 100, 120 MPa. As can be seen from the figure, there is a common relationship regardless of stress amplitudes between  $K_{i_{max}}$  and  $N_f$ . The lower  $K_{i_{max}}$ , the longer  $N_f$  becomes. The solid curve in the figure will be explained later.

In the present diecast magnesium alloy, the fatigue cracks initiated from the casting defects inside of the specimens with depths ranging from 50  $\mu\text{m}$  to 300  $\mu\text{m}$  from the specimen surfaces, just beneath the specimen surface. So we assume that the crack propagation law Eq. (3) for the surface cracks can be applied to the cracks initiated from the inner casting defects of the specimens because they locate at shallow portions, just beneath the specimen surface.

Integrating Eq. (3) from the initial maximum stress intensity factor  $K_{i_{max}}$  to the fatigue fracture toughness  $K_{fc}$  ( $7.0\text{MPam}^{1/2}$ ), the crack propagation lives  $N_p$  can be evaluated. For calculation of  $K_{i_{max}}$ , experimentally observed areas of the die-casting defects for the crack sources were utilized. In our previous studies [6], the crack initiation lives  $N_i$  are clarified to be about 10 % of total of fatigue lives  $N_f$ . The results indicate that  $N_f$  can be assumed as  $N_p$  by neglecting the crack initiation lives  $N_i$ . Figure 8 compares the evaluated relation  $K_{i_{max}}$  vs.  $N_f$  (solid curve) represented by Eq. (8) and experimental one, showing that a good correlation exists between them.

$$N_f \cong N_p = \left\{ \ln \left( \frac{K_{fc} - K_{th}}{K_{i_{max}} - K_{th}} \right) - K_{th} \left( \frac{1}{K_{fc} - K_{th}} - \frac{1}{K_{i_{max}} - K_{th}} \right) \right\} \times \left( \frac{0.5\sqrt{area}}{Y^2 A K_{i_{max}}^2} \right) \tag{8}$$

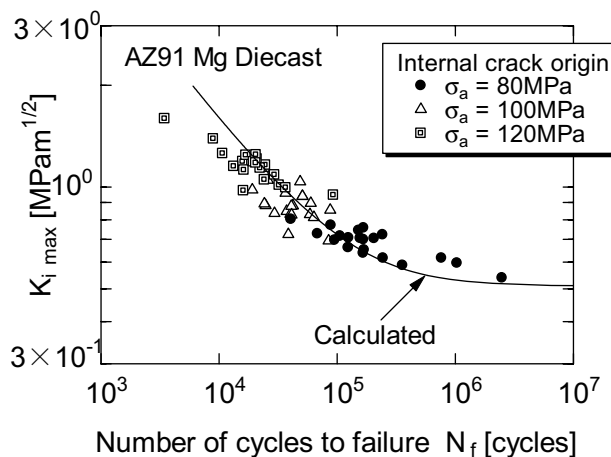


Fig. 8 Experimental and calculated relationship between  $K_{i_{max}}$  and  $N_f$ .

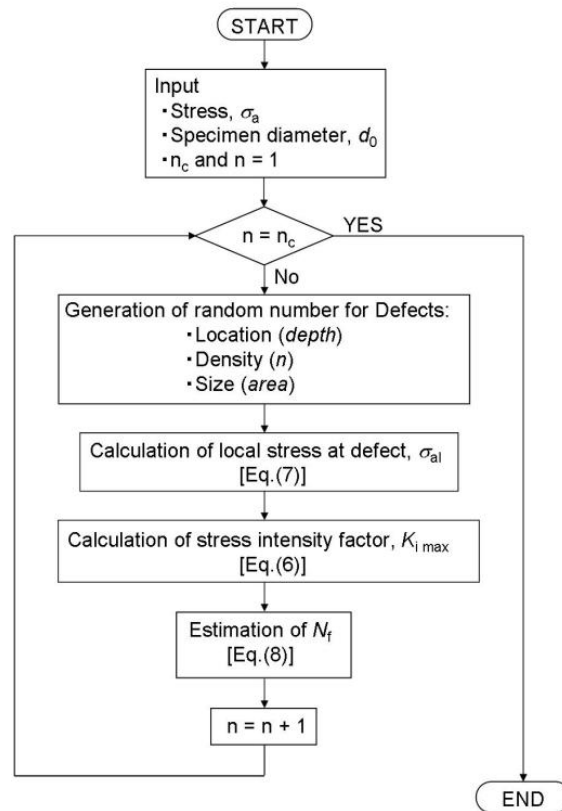


Fig.9 Flow chart of calculation and estimation of  $N_f$ .  $n_c$ : number of simulations.

#### 4. Estimation of the Distribution of fatigue lives using Computer Simulation

Monte Carlo simulation was conducted to evaluate the distribution of fatigue lives of the present diecast magnesium alloy on the basis of the distribution of the die-casting defects within the specimens. Figure 9 shows a flow chart of the computer simulation. In the simulation, Weibull random numbers were generated in a computer to simulate the defect sizes, *area* and defect densities, *n* for each of the fatigue specimen. Uniform random numbers were used for locations of the die-casting defects. Number of defects per specimen was calculated by multiplying the cross section area (28.26 mm<sup>2</sup>) to the above density *n*. Assuming these defects as cracks, the initial stress intensity factors  $K_i$  for the each of the defects were calculated, then the maximum value  $K_{i\ max}$  for each of the specimens can be determined. The fatigue life for the specimen can be evaluated using Eq. (8). One thousand trials ( $n_c$ : Number of Monte Carlo simulations) were conducted at the constant stress amplitude to realize the distribution of fatigue lives.



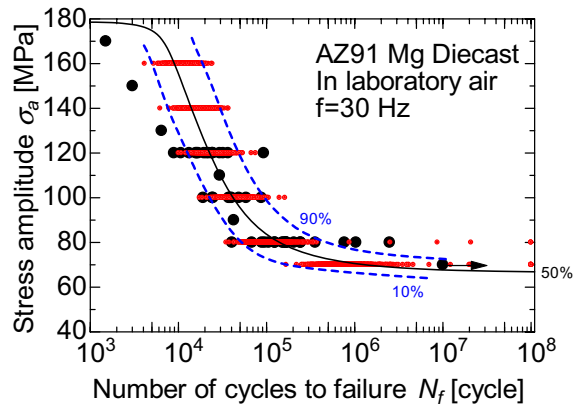
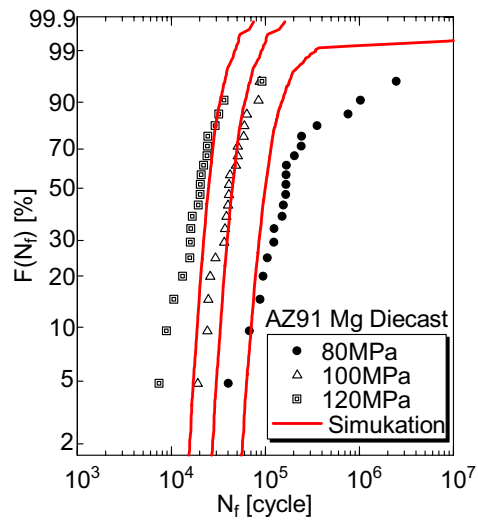
(a)  $S$ - $N$  curve(b)  $F(N_f)$ - $N_f$ 

Fig. 10 Weibull simulation data of AZ91 die-cast

The evaluated distribution of fatigue lives are compared with the experimental results in the  $S$ - $N$  curve (Fig. 10(a)) and in the distribution of fatigue lives (Fig. 10(b)). Good fits between them were observed in these figures. Therefore, distribution of fatigue lives for the diecast magnesium alloy is found to be estimated using both Monte Carlo simulation and surface fatigue crack propagation behavior. In the present simulation, the distributions of defect areas, their densities and their locations were taken into a consideration, but variation in the parameters involved in Eq. (3) were not considered.

## 5. Conclusions

Distributions of the fatigue lives were investigated using the diecast magnesium alloy AZ91, and following conclusions were reached.

- (1) Distributions of fatigue lives at the constant stress amplitudes can be represented by the Weibull distributions. Extents in the distributions for the higher stress amplitudes 100 and 120 MPa are almost identical to each other. However the scatter in the distribution of fatigue lives becomes larger at the lower stress amplitude of 80 MPa as compared with those at the higher stress amplitudes.
- (2) In the present diecast Mg alloy, sources of the fatigue cracks were clarified as the casting defects inside of the specimens regardless of the stress amplitudes. Their depths range from 50  $\mu\text{m}$  to 300  $\mu\text{m}$  from the specimen surfaces. The depth of the casting defects decreased with a decrease in the stress amplitude.
- (3) Distributions of the sizes and densities for the die-casting defects in the entire cross section of the specimen are represented by the three-parameters (Eq. (4)) and two-parameters (Eq. (5)) Weibull distributions.
- (4) In the log-log plot between the initial maximum stress intensity factors  $K_{imax}$  and fatigue lives  $N_f$ , there is a universal relationship between them regardless of stress amplitudes. The lower  $K_{imax}$ , the longer  $N_f$  becomes. Integrating the fatigue crack propagation law from the initial maximum stress intensity factor  $K_{imax}$  to the fatigue fracture toughness  $K_{fc}$ , the relation  $K_{imax}$  vs.  $N_f$  can be successfully evaluated.
- (5) Distribution of fatigue lives for the diecast AZ91 magnesium alloy is found to be estimated using both Monte Carlo simulation and surface fatigue crack propagation behaviour. In the simulation, the distributions of defect areas, their densities and their locations were taken into a consideration.

## Acknowledgement

The authors express their gratitude to NEDO, New Energy and Industrial Technology Development Organization in Japan, and Japan Aluminum Association for their financial support and their helps during the course of the present study.

## References

- [1] D. Mohr and R. Treitler, *Engineering Fracture Mechanics*, 75 (2008), pp.97-116
- [2] M. F. Horstemeyer, N. Yang, K. Gall, D. L. McDowell, J. Fan and P. M. Gullett, *Acta Materialia*, 52 (2004) pp.1327-1336
- [3] M. Avalle, G. Belingardi, M. P. Cavatorta and R. Doglione, *International Journal of Fatigue*, 24 (2002) pp.1-9
- [4] G. Murugan, K. Raghukandan, U. T. S. Pillai, B. C. Pai and K. Mahadevan, *Materials and Design*, 30 (2009) pp.2636-2641
- [5] Y. Murakami, *Metal fatigue: effects of small defects and nonmetallic inclusions*, Yokendo (1993)
- [6] S. Ishihara, Z. Nan and T. Goshima, *Materials Science and Engineering, A*, 468-470 (2007), pp.214-222